Fuel 233 (2018) 574–581

Contents lists available at ScienceDirect

Fuel

journal homepage: www.elsevier.com/locate/fuel

Full Length Article

One step synthesis of N-doped activated carbons derived from sustainable microalgae-NaAlg composites for CO_2 and CH_4 adsorption

Yaqi Wu[a,b], Zhaoan Chen[a], Yanan Liu[a], Yunpeng Xu[a,*], Zhongmin Liu[a,*]

[a] Dalian National Laboratory for Clean Energy, Dalian Institute of Chemical Physics, Chinese Academy of Sciences, Dalian 116023, China
[b] University of Chinese Academy of Sciences, Beijing 100049, China

GRAPHICAL ABSTRACT

Activated carbons derived from microalgae-NaAlg composites were prepared by one step activation under N_2 flow and exhibited efficient CO_2 and CH_4 adsorption capacities.

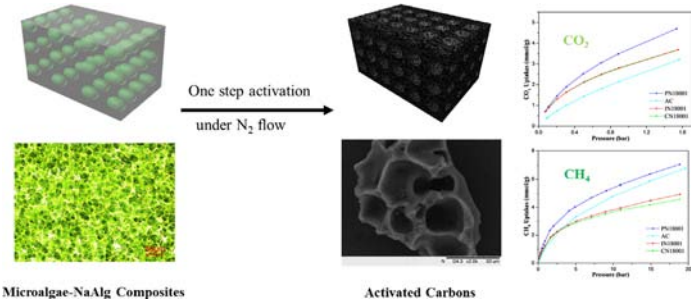

ARTICLE INFO

Keywords:
Microalgae-NaAlg composites
One step carbonization
N-doped activated carbons
CO_2 adsorption
CH_4 adsorption

ABSTRACT

N-doped activated carbons were obtained by using microalgae-sodium alginate (NaAlg) as renewable precursors due to the high nitrogen content of microalgae. One simple carbonization process with flowing N_2 gas only and no any other chemical agents or gases was used to prepare the activated carbons. Texture parameters, surface morphology and chemical properties of obtained activated carbons as well as the details of composition between microalgae and NaAlg have been investigated. By way of composition of microalgae and NaAlg, the tiny microalgae cells dispersed homogeneously inside the NaAlg and activated carbons with large specific surface areas over 1000 m^2/g were obtained. With high N content and appropriate pore size distributions, resulted activated carbons exhibited a very high CO_2 adsorption capacity of 3.75 mmol/g, 1 bar, 25 °C and CH_4 adsorption capacity of 7.27 mmol/g, 20 bar, 25 °C, which was much higher than commercial available coconut activated carbons (S_{BET} 1350 m^2/g). The results suggested that microalgae-NaAlg composites derived N-doped activated carbons to be promising adsorbents for CO_2 and CH_4 and the composition method may provide us new idea for greener activated carbon preparation.

1. Introduction

The continued demand and consumption of fossil fuels not only have raised concerns over the depleting of fossil energy reserves, excessive combustion of fossil fuels also have caused the rising concentration of atmospheric CO_2 which is the main culprit behind global warming (contributes to 60%) [1,2]. New sustainable and clean energies have been extensively required more than ever to reduce CO_2

* Corresponding authors.
E-mail addresses: xuyp@dicp.ac.cn (Y. Xu), liuzm@dicp.ac.cn (Z. Liu).

https://doi.org/10.1016/j.fuel.2018.06.094
Received 12 March 2018; Received in revised form 7 June 2018; Accepted 23 June 2018

emissions and relieve the shortage of energy. As a clean energy resource, CH_4 has attracted a great attention due to its many merits, such as considerable reserves, high caloric value and less carbon emissions etc. It is well known that adsorption is one of the most important techniques in the storage and utilization of methane, as well as an efficient way for CO_2 reduction [3,4]. Nevertheless, high efficient absorbents remain a barrier to practical and large-scale application for methane storage and CO_2 capture. To date, many adsorbents have been developed, such as zeolites, metal organic frameworks (MOFs), covalent organic frameworks (COFs), zeolitic imidazolate frameworks (ZIFs) and carbonaceous materials [5–12]. The low surface areas of zeolites and expensive cost of MOFs, COFs and ZIFs makes activated carbons to be one of the most significant and promising candidates owing to their high surface areas, stability and low cost [13–15]. Therefore, a large amount of investigations have been conducted and a broad array of carbon precursors have been used to prepare high performance activated carbon materials, such as a variety of shells (coconut shell, peanut shell, walnut shell, etc.), plenty of biomass (i.e. sawdust, macroalgae, olives stones, celtuce leaves), fish waste, metal organic aerogel, coal, petroleum coke and asphalts, etc. [16–27]. Particularly, activated carbon derived from biomass or naturally biological materials have received great attention due to the low cost, wide availability, environmental benignity and renewability.

Traditionally, there are several representative methods for the preparation of activated carbon, including chemical activation, physical activation and a combination of chemical and physical activation [28,29]. Chemical activation needs chemical agent like alkali, zinc chloride or acid to be involved which are unrecyclable, need to be washed out and unfriendly to the environment. Physical activation refers to the precursor first carbonized under inert atmosphere and then gasification under activating agent like water steam, CO_2, air, etc. Generally, activated carbon with surface areas higher than 1000 m^2/g must be obtained by either above methods. Thus, it will be a sustainable, energy-efficient and promising application that activated carbons derived from biomass precursors can be prepared only by one carbonization process under nitrogen flow without any other agent or gases.

As a unicellular photosynthetic microorganisms, microalgae have many advantages over other terrestrial biomass, including high photosynthetic efficiency, fast growth rate, high CO_2 fixation efficiency and no needing for arable land [30–32]. Microalgae are single-celled organisms that each microalgae cell is a micro-sized individual carbon source with high nitrogen content. Based on those features, microalgae are highly desirable precursors for preparation of activated carbon materials. However, only a few researchers have tried to utilize microalgae to prepare activated carbon materials. Wang et al. obtained cyanobacteria derived activated carbons as high performance electrode in symmetric supercapacitor with KOH treatment [33]. While Tsai et al. prepared activated carbons by using chlorella-based microalgal residue as precursor with flowing N_2 and CO_2 gases [34]. There remain significant challenges in the utilization of microalgae to prepare activated carbon with high surface area and simple activation process due to the aggregation and fusion of microalgae cells in the pyrolysis process.

In this work, we have developed a facile method by composited microalgae and sodium alginate (NaAlg) together as sustainable precursors to prepare activated carbons for desirable CO_2 and CH_4 adsorption. Sodium alginate (NaAlg) with a chemical formula of $(C_6H_7NaO_6)_n$ is quite abundant in nature and has been extensively used as binder, cross-linking agent, component of drug delivery system, additives, in food, pharmaceutical and therapeutic applications [35–37]. Therefore, NaAlg can be used as a special binder to adhere and isolate microalgae cells which can take the advantage of tiny microalgae carbon source and be carbon source at the same time. Several microalgae (Chorella, Isochrysis and Platymonas subcordiformis) were investigated to composite with NaAlg. By the special composition, it has achieved an interesting composition effect that for the composites both surface area and pore volume are much higher than the NaAlg and microalgae separately. Benefiting from the merits of abundant micropores, appropriate pore size distribution and high nitrogen content, the obtained activated carbon materials exhibit considerable CO_2 and CH_4 uptakes. The mechanism of the composition effect and the reason of high CO_2 and CH_4 adsorption capacities of the activated carbons were also discussed.

2. Experimental

2.1. Materials

Chorella, Isochrysis and Platymonas subcordiformis powder were obtained from Marine bioengineering group of Dalian Institute Chemical Physics, Chinese Academy of Sciences. Granular coconut shell activated carbon (AC) was purchased from Fujian Xinsen Carbon Co., Ltd.

2.2. Preparation of microalgae-NaAlg composites.

To prepare the composites, microalgae (Chorella, Isochrysis and Platymonas subcordiformis) powder was well dispersed in a certain amount of deionized water. Then sodium alginate was added in the above solution and stirred homogenously. The resulting gel solution was poured into a culture dish and dried at ambient conditions. The microalgae (Chorella, Isochrysis and Platymonas subcordiformis)-NaAlg composites we got were donated as C-NaAlg, I-NaAlg and P-NaAlg, respectively.

2.3. Preparation of activated carbons.

Dry composite was placed in a quartz reactor inside a tube furnace. The whole pyrolysis process was carried out under N_2 flow (120 mL/min). Firstly, the composite was heated to 500 °C with a heating rate of 2.5 °C/min at a residence time of 1 h and then to the activation temperature with a heating rate of 5 °C/min at a residence time of 1 h. After activation, the samples were cooled down to ambient temperature naturally under nitrogen atmosphere. The resultant samples were washed three times with 1 M hydrochloric acid and then with deionized water to neutral. Finally, the samples were dried at 110 °C for 12 h. Thus, for a typical activated carbon which prepared with a Chorella/NaAlg mass ratio of 1/2 and has been pyrolyzed at 800 °C for 1 h, was denominated as CN28001 (for Chorella or NaAlg individually, it would be C8001 or N8001). The yield of the typical samples are listed in Table S1.

Supplementary data associated with this article can be found, in the online version, at https://doi.org/10.1016/j.fuel.2018.06.094.

2.4. Characterizations

Nitrogen adsorption-desorption isotherms, specific surface areas and porosity of samples were measured by a volumetric adsorption analyzer (Micromeritics, ASAP 2020, USA) using nitrogen as adsorbate at −196 °C and samples were degassed under vacuum at 250 °C for 4 h. The specific surface area (S_{BET}) was calculated by the Brunauer-Emmett-Teller (BET) method from the data on N_2 isotherm in the relative pressure (p/p_0) range of 0.05–0.25. The total pore volume (V_t) was estimated to be the liquid volume of N_2 at a high relative pressure (p/p_0) of 0.98. The micropore surface areas (S_{micro}) and micropore volume (V_{micro}) of resulted samples were obtained via t-plot method, a plot of the statistical thickness (t) versus the relative pressure [38]. The pore size distributions were deduced from Density Functional Theory (DFT). Microphotographs were taken by Nikon Eclipes (NI-U, Japan) with high-definition color camera head (DS-Fi2) to observe the composited details of the precursors. Scanning electron microscopy (SEM) images were measured on Hitachi TM3000 and Hitachi SU8020 cold field emission scanning electron microscope, respectively.

Table 1
Surface area (S_{BET}, m^2/g) of activated carbons derived from NaAlg, microalgae and microalgae-NaAlg composites at different activation temperatures.[1]

Sample	600 °C	650 °C	700 °C	750 °C	800 °C
NaAlg	171	412	417	583	595
Chorella	30	32	24	32	65
C-NaAlg composite	129	346	514	642	684
Isochrysis	51	38	61	138	53
I-NaAlg composite	254	609	539	522	736
Platymonas subcordiformis	284	453	459	601	627
P-NaAlg composite	334	509	909	922	1032

[1] All composites with a microalgae/NaAlg mass ratio of 1:1. The resulting activated carbons produced at a certain pyrolysis temperature for holding time of 1 h using N_2 gas (flow rate 120 mL/min).

Thermogravimetry (TG) and differential thermal analysis (DTA) were carried out using a SDT Q600 (TA Instruments-Waters LLC, USA) in the atmosphere of nitrogen. The nitrogen (N) content of resulted activated carbons were obtained by an elemental analyzer (Elementar; Model: vario EL cube; Germany). Both CH_4 and CO_2 uptake measurements were performed by volumetric methods (Quantachrome, iSorb HP2) under the pressure range of 0–20 bar at 25 °C. The purity of the used CH_4 and CO_2 were both 99.999%.

3. Result and discussion

3.1. Activated carbons from NaAlg, microalgae and microalgae-NaAlg composites

NaAlg, microalgae (Chorella, Isochrysis and Platymonas subcordiformis) and their composites with a microalgae/NaAlg mass ratio of 1:1 were used as precursors for activated carbons respectively. Pore parameters of resulted samples at the temperature of 600–800 °C are present in Tables 1 and 2. It can be seen that activated carbons derived from Chorella and Isochrysis present BET surface areas lower than 100 m^2/g without a clear trend as the temperature increases. The S_{BET} increased with the pyrolysis temperature increasing for samples obtained from NaAlg, C-NaAlg, I-NaAlg, Platymonas subcordiformis and P-NaAlg. With the temperature increasing, S_{BET} of samples from Platymonas subcordiformis increased from 284 to 627 m^2/g and S_{BET} of samples from NaAlg increased from 171 to 595 m^2/g. While for samples from microalgae-NaAlg composites, S_{BET} of C-NaAlg, I-NaAlg and P-NaAlg increased from 129, 254 and 334 m^2/g to 684, 736 and 1032 m^2/g, respectively. From detailed pore parameters of resulted activated carbons at 800 °C in Table 2, it can be seen that activated carbons derived from composites have abundant micropores and their S_{micro} are higher than that of activated carbons obtained from NaAlg and microalgae separately. Among the three microalgae, Platymonas subcordiformis derived activated carbons achieved a much higher S_{BET} and S_{micro} than Chorella and Isochrysis whether on their own or composited with NaAlg. The highest S_{BET} and total pore volume of P-NaAlg derived activated carbons were up to 1032 m^2/g and 0.61 cm^3/g, respectively. While under the same conditions, S_{BET} and total pore volume of activated carbons obtained from NaAlg were only 595 m^2/g and 0.34 cm^3/g and those obtained from Platymonas subcordiformis were only 627 m^2/g and 0.38 cm^3/g, respectively. Interestingly, for all these microalgae-NaAlg composites, the resulted activated carbons have much higher surface areas and total pore volume than those samples obtained from NaAlg and microalgae individually, and we named it as “composition effect”.

Table 2
Textural parameters of activated carbons derived from NaAlg, microalgae, microalgae-NaAlg composites and AC at activation temperature of 800 °C.[1]

Sample	S_{BET} m^2/g	S_{micro} m^2/g	V_t mL/g	V_{micro} mL/g
N8001	595	378	0.34	0.18
C8001	65	32	0.1	0.01
CN18001	684	579	0.39	0.27
I8001	53	24	0.09	0.01
IN18001	736	621	0.42	0.29
P8001	627	435	0.38	0.21
PN18001	1032	878	0.61	0.41
PN28001	945	758	0.54	0.35
PN48001	965	743	0.53	0.34
AC	1350	720	0.69	0.32

[1] The resulting activated carbons produced at 800 °C for holding time of 1 h using N_2 gas (flow rate 120 mL/min).

The N_2 adsorption-desorption isotherms and pore size distributions deduced from DFT method of CN18001, IN18001 and PN18001 are shown in Fig. 1a and b, respectively. Those isotherms are typically type IV isotherms with hysteresis loops of varying sizes in the desorption isotherm, which indicated that there are not merely micropores, but also with a portion of mesopores and macropores existed in those activated carbons. The pore size distributions of these samples mainly concentrate on the range of 0.5–1.5 nm. Fig. 2 shows the SEM images of P18001, N18001 and PN18001. P8001 (Fig. 2a and b) seems that the tissue structure has not been destroyed severely and Platymonas subcordiformis cells trend to cross-linked and fused together during the carbonization process. N8001(Fig. 2c and d) has more porous surface while composite with Platymonas subcordiformis (PN18001, Fig. 2e and f), it can be seen clearly that there are obvious micro-sized holes left by Platymonas subcordiformis cells which seems fused together with NaAlg after pyrolysis and it can be seen many small pores in its cross sectional views under high magnification. SEM images and N_2 adsorption-desorption isotherms of CN18001 and IN18001 (Figs. S1 and S2) has shown similar isotherm type and porous surface morphology to PN18001.

3.2. The composition effect

Taking the characteristics of the above three microalgae into account, the composition effect was further studied by Platymonas subcordiformis and NaAlg composites. The mass ratios of the P-NaAlg composites were changed from 1:1 to 1:2, 1:4. The microphotographs of microalgae-NaAlg composites in the form of gel solution and dry form are shown in Fig. 3. Platymonas subcordiformis is a unicellular specie with sizes around 10–20 μm. As shown in Fig. 3a–c, it is quite clear that microalgae cells were well dispersed in the transparent gel solution and corresponding densities varied from the mass ratios. After the water has been evaporated and the solution has been shrunk, those microalgae cells were wrapped by NaAlg and condensed uniformly (Fig. 3d–f). SEM images of resulted activated carbons (PN18001, PN28001 and PN48001) are presented in Fig. 3g–i. It was clearly shown that many micron-sized pores appeared in the surface of the obtained samples which are highly in accordance with the size of Platymonas subcordiformis cells. The pore parameters of the resulted carbon materials are also presented in Table 2. Activated carbons derived from microalgae-NaAlg composites displayed different porosity characteristics with different microalgae/NaAlg mass ratios. The S_{BET} and S_{micro} of resulted activated carbons decreased slightly from 1032, 878 m^2/g to 945, 758 m^2/g and 965 m^2/g, 743 m^2/g, respectively, when the microalgae/NaAlg mass ratio decreased from 1:1 to 1:2 and 1:4. Although the surface area decreased slightly as the microalgae ratio decreasing, the composition effect still existed. It can be concluded that the composition of microalgae and NaAlg would facilitate the formation of pores especially micropores during the carbonization process.

Herein, we put forward a detailed mechanism of the composition effect in microalgae-NaAlg composites which can be illustrated as Scheme 1 shown (Platymonas subcordiformis-NaAlg composite was chose as model). On one hand, microalgae and NaAlg are essentially different carbon sources. NaAlg with a chemical formula of

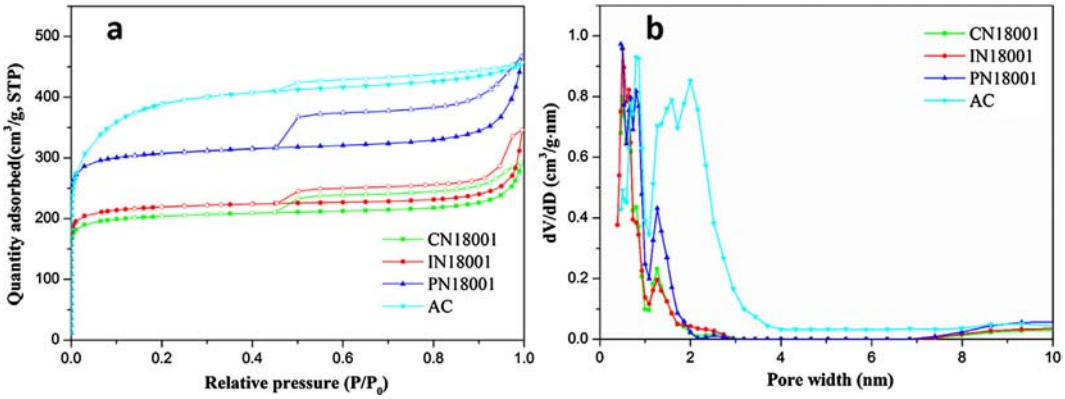

Fig. 1. (a) N_2 adsorption-desorption isotherms (full symbols: adsorption; open symbols: desorption) and (b) pore size distributions of activated carbons from microalgae-NaAlg composite and commercially available activated coconut carbon (AC).

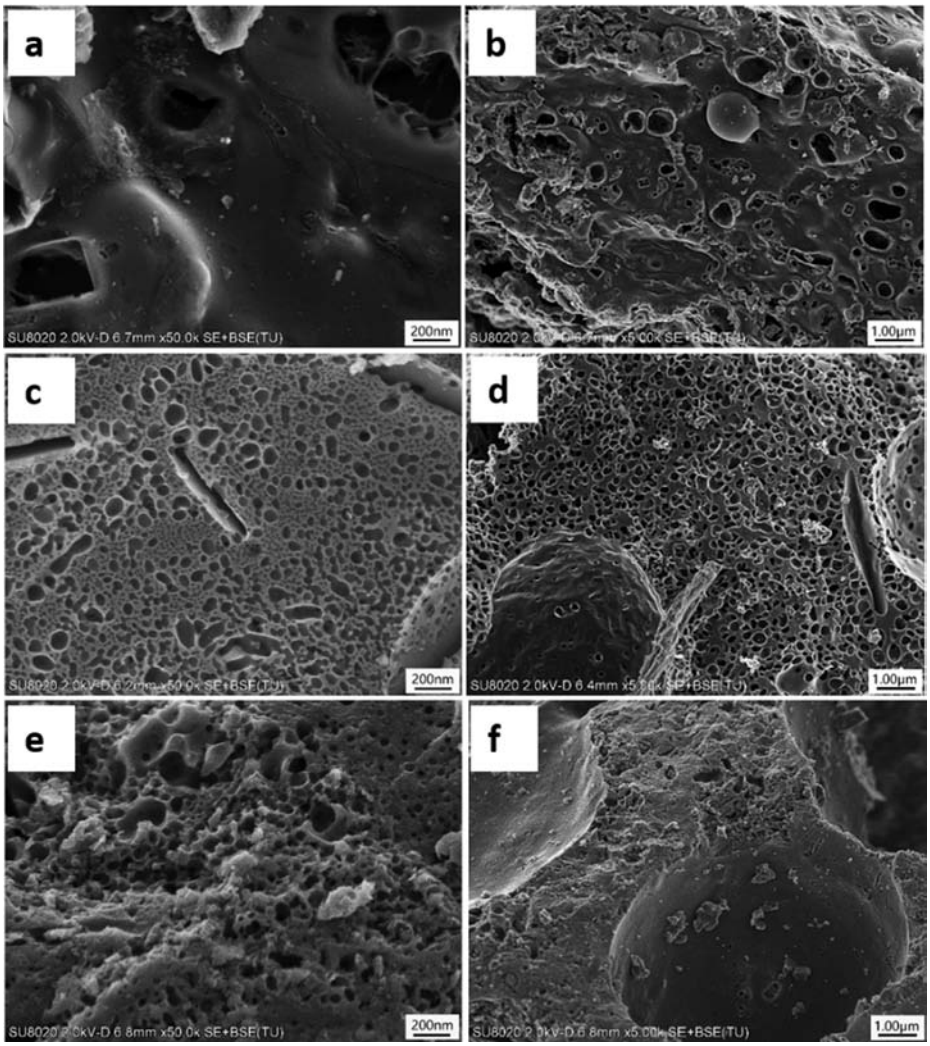

Fig. 2. SEM images of the materials studied. (a, b) P8001 ×50.0k, ×5.0k; (c, d) N8001 ×50.0k, ×5.0k; (e, f) PN18001 ×50.0k, ×5.0k.

$(C_6H_7NaO_6)_n$ is a kind of pure biopolymer which can dissolve in water. Microalgae are single-celled organisms, mainly composed of proteins, lipids, carbohydrates etc. When the heterogeneous Platymonas subcordiformis cells embedded in the homogenous NaAlg, it will lead to an increase in heterogeneity and irregular pyrolysis of the carbon precursor thus facilitate to develop abundant pores. On the other hand, there appears a big difference between the thermal behaviors of Platymonas subcordiformis, NaAlg and P-NaAlg composite (with the microalgae/NaAlg mass ratio of 1:1) according to the TG results (Fig. 4a and b). During the pyrolysis process, there was a sharp exothermic peak around 250 °C corresponding to the fast decomposition of NaAlg and a relatively slower decomposition of Platymonas subcordiformis appears around 300 °C. When they composited, those microalgae cells were isolated by NaAlg, the thermal behavior was different from when they fusing together. And the fast decomposed NaAlg wrapped the slower decomposed Platymonas subcordiformis which may result in more

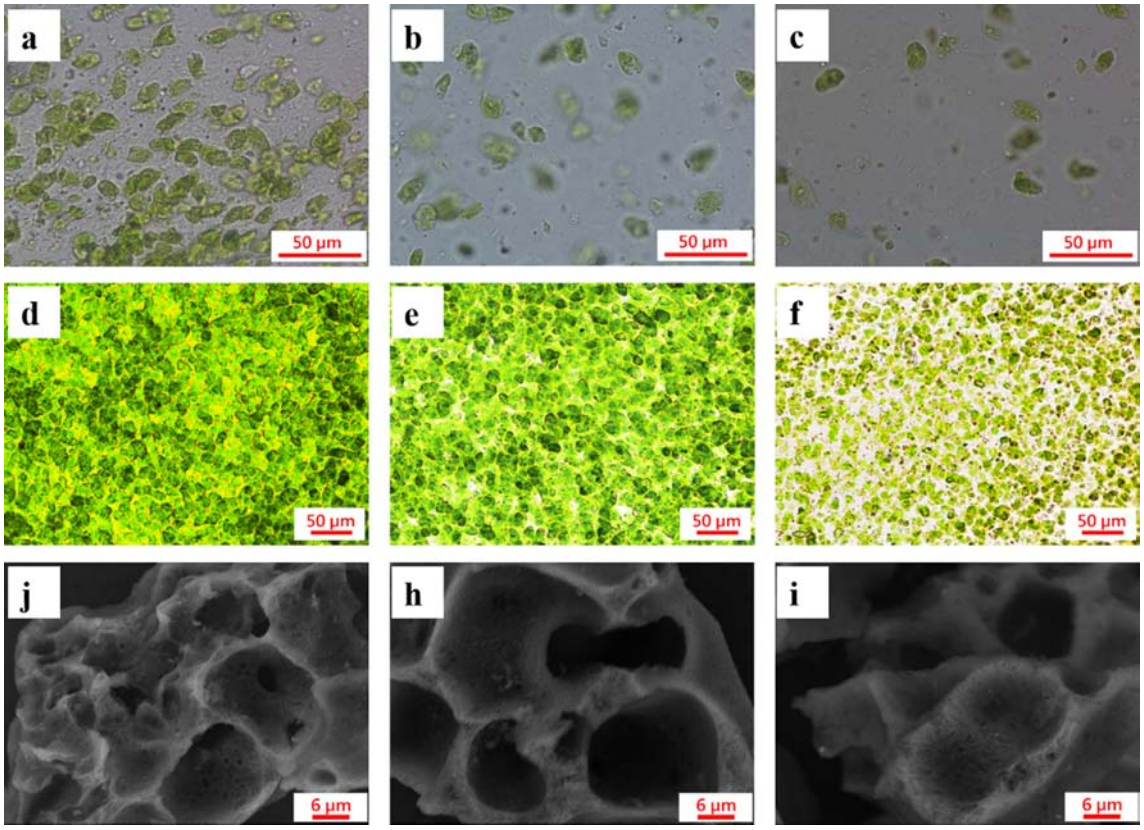

Fig. 3. Microphotographs of P-NaAlg composites in the form of gel solution (a–c) and dry film (d–f). (a, d) P-NaAlg composite with a microalgae/NaAlg mass ratio of 1:1 using 40× and 20× objective lens, respectively. (b, e) P-NaAlg composite with a microalgae/NaAlg mass ratio of 1:2 using 40× and 20× objective lens, respectively. (c, f) P-NaAlg composite with a microalgae/NaAlg mass ratio of 1:4 using 40× and 20× objective lens, respectively. (j, h and i) SEM images of PN18001, PN28001 and PN48001, ×3.0k, respectively.

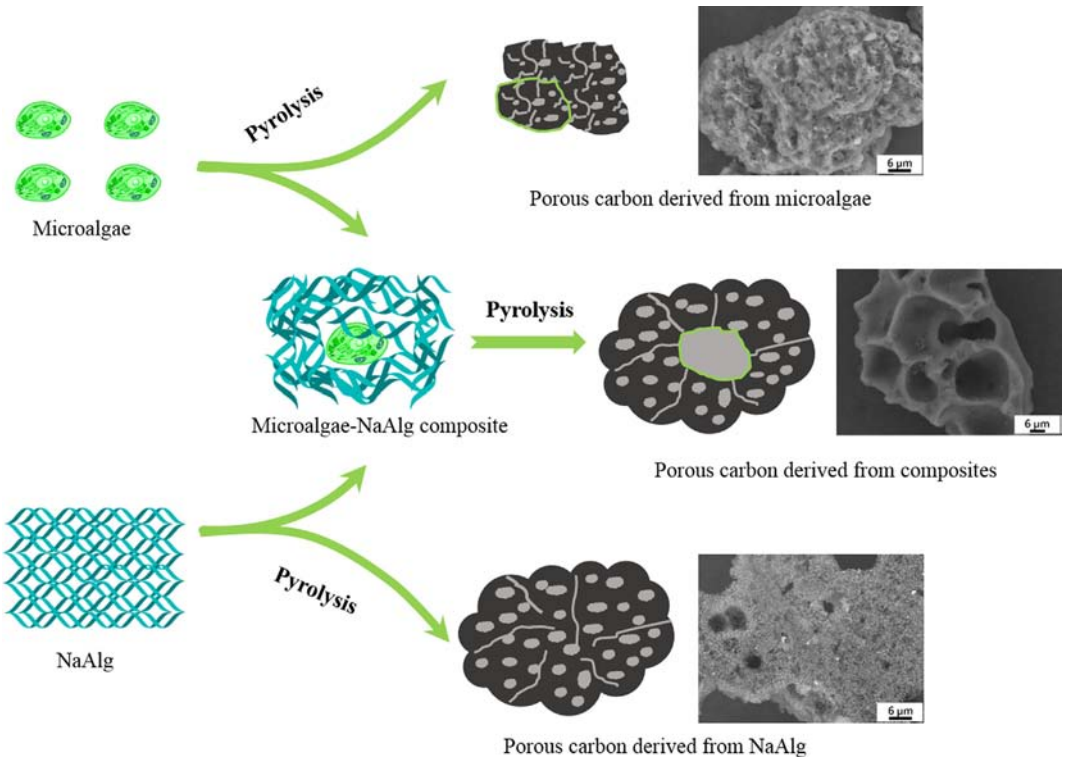

Scheme 1. Schematic illustration of the composition effect with correspondent microphotographs and SEM images.

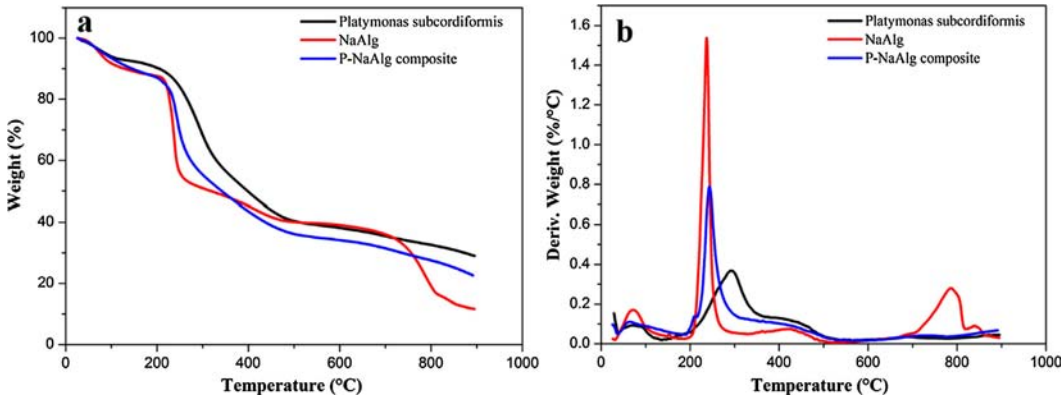

Fig. 4. (a) TG and (b) DTG curves of Platymonas subcordiformis, NaAlg and P-NaAlg composite. The microalgae/NaAlg mass ratio of P-NaAlg was 1:1.

defect sites and especially in the junction of the two carbon sources, the permeation and fusion between them may also have mutual promoted effect and thus generated more pores and larger surface areas. Also, from the TG and DTG curves of P-NaAlg composite, it can be seen that its exothermic peaks and thermal decomposition temperatures were unique and not a simple overlay of Platymonas subcordiformis and NaAlg. As discussed above, we can conclude that the essential difference, embedding effect and their own pyrolysis peculiarities of Platymonas subcordiformis and NaAlg contribute to the composition effect, which will facilitate the formation of high porosity of activated carbons. The new thermal decomposition behavior of P-NaAlg composite would also be helpful in understanding the composition effect.

3.3. Gas adsorption performance

3.3.1. Adsorption performance of CO_2

Previous researches have revealed that a highly microporous structure with a large surface area is desirable for CO_2 adsorption [26,39,40]. In this work, we have tested the CO_2 adsorption capacity of CN18001, IN18001 and PN18001. Commercially granular coconut activated carbon (AC) has similar S_{BET} and S_{micro} with samples in this work while it was generally prepared by complicated chemical or physical activation process. Therefore, we also tested CO_2 uptakes of AC for comparison and its N_2 adsorption-desorption isotherms and pore size distributions deduced from DFT method are also present in Fig. 1a and b. It can be seen that the N_2 adsorption-desorption isotherms of AC presents a small type H4 hysteresis loop attributing to its narrow slit pores. The textural parameters of AC are also listed in Table 2. The CO_2 adsorption performance of CN18001, IN18001, PN18001 and AC are illustrated in Fig. 5a and b. It can be seen that PN18001 exhibited the highest CO_2 uptake of 3.75 mmol/g, 1 bar, and 25 °C among the four activated carbons followed by IN18001, CN18001 and AC. As CO_2 is essentially slight acidic, it has been demonstrated that absorbents with nitrogen introduced into its framework can greatly enhance the CO_2 adsorption capacity [18,19,41–43]. The nitrogen content of microalgae, NaAlg, microalgae-NaAlg composite resulted porous carbons and AC are presented in Table 3. It can be seen that the high nitrogen content of Chorella (8.34 wt%), Isochrysis (6.49 wt%) and Platymonas subcordiformis (6.97 wt%) make them desirable nitrogen sources at the same time which resulted in N-rich activated carbons with considerable nitrogen contents of 4.17 wt% (CN18001), 3.61 wt% (IN18001) and 3.34 wt% (PN18001), respectively. While the nitrogen content of AC is merely 0.3 wt%. Therefore, it is easy to understand that the initial CO_2 uptakes of microalgae-NaAlg composite derived activated carbons were much higher than that of AC because of their high nitrogen content in spite of their lower surface areas. However, with the pressure increasing, the CO_2 adsorption capacity of AC exceeds CN18001, IN18001 and PN18001 gradually. This result is expected because AC has higher surface area and pore volume. CO_2 uptakes of samples at high pressures differ from low pressures which for one thing, the adsorption based on acid–base interactions between basic N-groups and acidic CO_2 is monolayer adsorption which would be saturated as pressure increases, for another thing, large micropores/small mesopores play important roles in CO_2 adsorption at high pressures [44,45]. The nitrogen introduced by microalgae results in the high nitrogen of

Table 3
Nitrogen content of microalgae, NaAlg, microalgae-NaAlg composite resulted porous carbons and AC.[1]

Sample	C	I	P	NaAlg	CN18001	IN18001	PIN18001	AC
N (wt%)	8.34	6.49	6.97	neg.	4.17	3.61	3.34	0.3

[1] C-Chorella, I-Isochrysis, P-Platymonas subcordiformis.

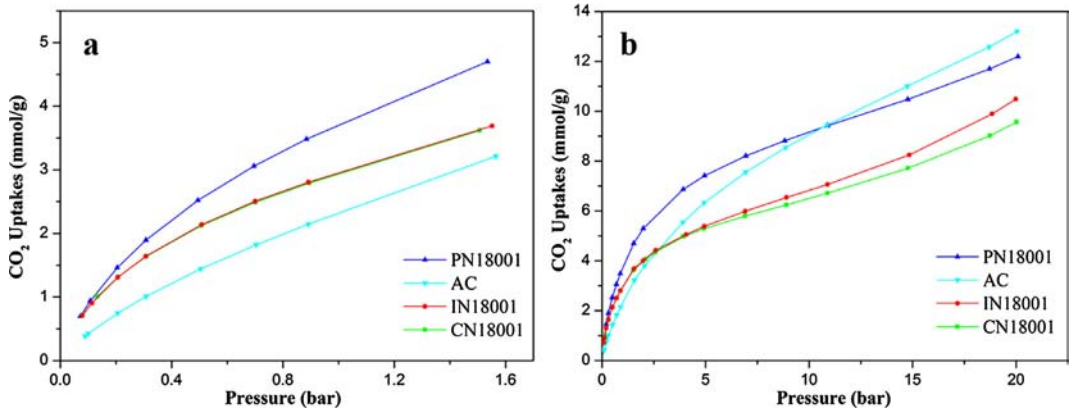

Fig. 5. CO_2 adsorption isotherms of PN18001, IN18001, CN18001 and AC at 25 °C. (a) the pressures up to 1.5 bar, and (b) the corresponding adsorption up to 20 bar.

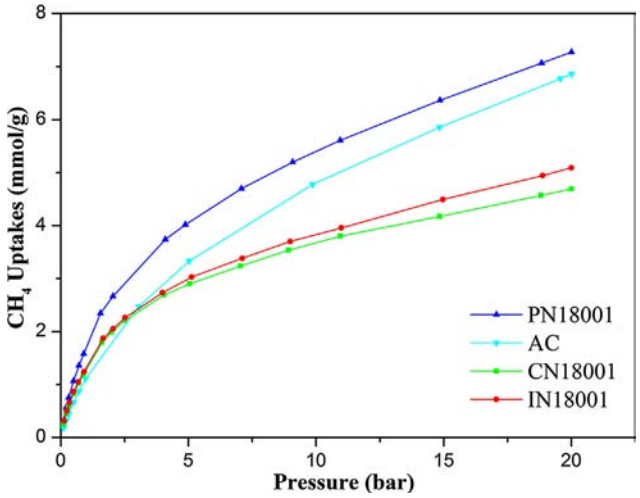

Fig. 6. CH_4 adsorption isotherms of PN18001, IN18001, CN18001 and AC at 25 °C and the pressures up to 20 bar.

the corresponding activated carbons which can greatly enhance their efficient CO_2 adsorption capacities.

3.3.2. Adsorption performance of CH_4

The CH_4 adsorption isotherms of PN18001, IN18001, CN18001 and AC from 0 to 20 bar by volumetric method are shown in Fig. 6. For methane adsorbent materials, both high enough surface areas and appropriate pore textures including microporosity and pore size distributions are necessary to insure their adsorption performance [46,47]. Many theoretical simulation studies have indicated that the optimal pore size for methane adsorption is micropores at approximately 1.1–1.5 nm [48–51] and relevant pore size distributions (Fig. 1b) of PN18001, IN18001 and CN18001 is located in this range. And Lozano-Castello et al. also demonstrated that methane adsorption capacity not only depends on the micropore volume but also strongly depends on the micropore size distribution [52]. From the textural properties and porosity parameters discussed above, we can deduce that PN18001 may exhibit larger methane uptakes than the other three. It is indeed that PN18001 showed the highest CH_4 adsorption capacities. It is well-known that micropores are of great benefit for methane adsorption with the same surface areas. However, methane uptake also can keep increasing within large micropores and small mesopores at relative high pressures due to the condensation effect [2]. Therefore, it can be expected that with pressure increasing, the CH_4 uptakes of AC was getting closer to PN18001 and the differences of CH_4 uptakes between AC, IN18001 and CN18001 were more obvious. Sample PN18001 with a high BET surface area of 1032 m^2/g exhibited a high CH_4 adsorption capacity of 7.27 mmol/g, 20 bar, and 25 °C. Appropriate micropore size distributions have great effects on CH_4 uptake and large amount of small mesopores also can make contributions to methane adsorption especially under high pressures.

4. Conclusion

In this work, microalgae-NaAlg composites were initiatively used as sustainable precursors to obtain activated carbons with high CO_2 and CH_4 adsorption performance. Activated carbons were prepared by one simple carbonization process with flowing N_2 gas only and no any other chemical agents or gases was used. Sample PN18001 exhibited a high BET surface area of 1032 m^2/g. By composition, a composition effect was found between microalgae and NaAlg that activated carbons derived from composites show much higher S_{BET} and V_t than those from NaAlg and microalgae individually. A detailed mechanism was investigated that the two heterogeneous carbon source of microalgae and NaAlg, the tiny microalgae cells embedded by NaAlg and different thermal behaviors of microalgae and NaAlg contribute to the higher surface area of composite-derived activated carbons. With the introduction of microalgae, it would facilitate the formation of porous structures and result in activated carbons with high nitrogen content. Thus make these materials to be efficient adsorbents for CO_2 and CH_4 which the CO_2 and CH_4 uptakes was much higher than AC even with a lower surface area. Sample PN18001 showed a very high CO_2 adsorption capacity of 3.75 mmol/g, 1 bar, 25 °C and CH_4 adsorption capacity of 7.27 mmol/g, 20 bar, and 25 °C. The results implied that abundant micropores, appropriate pore size distributions and high nitrogen content of activated carbons play very important roles in CO_2 and CH_4 adsorption besides high surface areas. Furthermore, the composition effect found in microalgae-NaAlg composites provides us new idea for greener activated carbon preparation. The resulted activated carbons were not only limited to be used as CO_2 and CH_4 adsorbent, but also expected to be applied to fields ranging from electrode to catalyst.

Acknowledgement

This work was supported by the National Key Research and Development Program of China (2016YFB0301603).

References

[1] Yu KMK, Curcic I, Gabriel J, Tsang SCE. Recent advances in CO_2 capture and utilization. ChemSusChem 2008;1(11):893–9.
[2] Cai J, Qi J, Yang C, Zhao X. Poly(vinylidene chloride)-based carbon with ultrahigh microporosity and outstanding performance for CH_4 and H_2 storage and CO_2 capture. ACS Appl Mater Interfaces 2014;6(5):3703–11.
[3] Wang Q, Luo J, Zhong Z, Borgna A. CO_2 capture by solid adsorbents and their applications: current status and new trends. Energy Environ Sci 2011;4(1):42–55.
[4] Makal TA, Li J-R, Lu W, Zhou H-C. Methane storage in advanced porous materials. Chem Soc Rev 2012;41(23):7761–79.
[5] Darunte LA, Oetomo AD, Walton KS, Sholl DS, Jones CW. Direct air capture of CO_2 using amine functionalized MIL-101(Cr). ACS Sustainable Chem Eng 2016;4(10):5761–8.
[6] Cavenati S, Grande CA, Rodrigues AE. Adsorption equilibrium of methane, carbon dioxide, and nitrogen on zeolite 13× at high pressures. J Chem Eng Data 2004;49(4):1095–101.
[7] Saha D, Bao Z, Jia F, Deng S. Adsorption of CO_2, CH_4, N_2O, and N_2 on MOF-5, MOF-177, and zeolite 5A. Environ Sci Technol 2010;44(5):1820–6.
[8] Furukawa H, Yaghi OM. Storage of hydrogen, methane, and carbon dioxide in highly porous covalent organic frameworks for clean energy applications. J Am Chem Soc 2009;131(25):8875–83.
[9] Ashourirad B, Sekizkardes AK, Altarawneh S, El-Kaderi HM. Exceptional gas adsorption properties by nitrogen-doped porous carbons derived from benzimidazole-linked polymers. Chem Mater 2015;27(4):1349–58.
[10] Himeno S, Komatsu T, Fujita S. High-pressure adsorption equilibria of methane and carbon dioxide on several activated carbons. J Chem Eng Data 2005;50(2):369–76.
[11] Banerjee R, Phan A, Wang B, Knobler C, Furukawa H, Keeffe M, et al. High-throughput synthesis of zeolitic imidazolate frameworks and application to CO_2 capture. Science 2008;319(5865):939.
[12] Bourrelly S, Llewellyn PL, Serre C, Millange F, Loiseau T, Férey G. Different adsorption behaviors of methane and carbon dioxide in the isotypic nanoporous metal terephthalates MIL-53 and MIL-47. J Am Chem Soc 2005;127(39):13519–21.
[13] Marco-Lozar JP, Kunowsky M, Suárez-García F, Carruthers JD, Linares-Solano A. Activated carbon monoliths for gas storage at room temperature. Energy Environ Sci 2012;5(12):9833.
[14] Wang Y, Ercan C, Khawajah A, Othman R. Experimental and theoretical study of methane adsorption on granular activated carbons. AlChE J 2012;58(3):782–8.
[15] Castro-Muniz A, Suarez-Garcia F, Martinez-Alonso A, Tascon JM, Kyotani T. Energy storage on ultrahigh surface area activated carbon fibers derived from PMIA. ChemSusChem 2013;6(8):1406–13.
[16] Chen J, Yang J, Hu G, Hu X, Li Z, Shen S, et al. Enhanced CO_2 capture capacity of nitrogen-doped biomass-derived porous carbons. ACS Sustainable Chem Eng 2016;4(3):1439–45.
[17] Ahmad M, Lee SS, Dou X, Mohan D, Sung J-K, Yang JE, et al. Effects of pyrolysis temperature on soybean stover- and peanut shell-derived biochar properties and TCE adsorption in water. Bioresour Technol 2012;118:536–44.
[18] Hao G-P, Li W-C, Qian D, Lu A-H. Rapid synthesis of nitrogen-doped porous carbon monolith for CO_2 capture. Adv Mater 2010;22(7):853–7.
[19] To JWF, He J, Mei J, Haghpanah R, Chen Z, Kurosawa T, et al. Hierarchical N-doped carbon as CO_2 adsorbent with high CO_2 selectivity from rationally designed polypyrrole precursor. J Am Chem Soc 2016;138(3):1001–9.
[20] Sevilla M, Fuertes AB. Sustainable porous carbons with a superior performance for CO_2 capture. Energy Environ Sci 2011;4(5):1765–71.
[21] Ferrera-Lorenzo N, Fuente E, Suárez-Ruiz I, Ruiz B. Sustainable activated carbons of

macroalgae waste from the Agar-Agar industry. Prospects as adsorbent for gas storage at high pressures. Chem Eng J 2014;250:128–36.
[22] Sivadas DL, Vijayan S, Rajeev R, Ninan KN, Prabhakaran K. Nitrogen-enriched microporous carbon derived from sucrose and urea with superior CO_2 capture performance. Carbon 2016;109:7–18.
[23] Fadhil AB, Ahmed AI, Salih HA. Production of liquid fuels and activated carbons from fish waste. Fuel 2017;187:435–45.
[24] Zhang H, Zhao Z, Liu Y, Liang J, Hou Y, Zhang Z, et al. Nitrogen-doped hierarchical porous carbon derived from metal-organic aerogel for high performance lithium-sulfur batteries. J Energy Chem 2017;26(6):1282–90.
[25] Wang R, Wang P, Yan X, Lang J, Peng C, Xue Q. Promising porous carbon derived from celtuce leaves with outstanding supercapacitance and CO_2 capture performance. ACS Appl Mater Interfaces 2012;4(11):5800–6.
[26] Jalilov AS, Li Y, Tian J, Tour JM. Ultra-high surface area activated porous asphalt for CO_2 capture through competitive adsorption at high pressures. Adv Energy Mater 2017;7(1):100693.
[27] Plaza MG, Pevida C, Arenillas A, Rubiera F, Pis JJ. CO_2 capture by adsorption with nitrogen enriched carbons. Fuel 2007;86(14):2204–12.
[28] Cardoso B, Mestre AS, Carvalho AP, Pires J. Activated carbon derived from cork powder waste by KOH activation: preparation, characterization, and VOCs adsorption. Ind Eng Chem Res 2008;47(16):5841–6.
[29] Wang H, Gao Q, Hu J. High hydrogen storage capacity of porous carbons prepared by using activated carbon. J Am Chem Soc 2009;131(20):7016–22.
[30] de Morais MG, Costa JAV. Carbon dioxide fixation by Chlorella kessleri, C. vulgaris, Scenedesmus obliquus and Spirulina sp. cultivated in flasks and vertical tubular photobioreactors. Biotechnol Lett 2007;29(9):1349–52.
[31] Chae SR, Hwang EJ, Shin HS. Single cell protein production of Euglena gracilis and carbon dioxide fixation in an innovative photo-bioreactor. Bioresour Technol 2006;97(2):322–9.
[32] Sakai N, Sakamoto Y, Kishimoto N, Chihara M, Karube I. Chlorella strains from hot springs tolerant to high temperature and high CO_2. Energy Convers Manage 1995;36(6):693–6.
[33] Wang K, Cao Y, Wang X, Fan Q, Gibbons W, Johnson T, et al. Pyrolytic cyanobacteria derived activated carbon as high performance electrode in symmetric supercapacitor. Energy 2016;94:666–71.
[34] Chang YM, Tsai WT, Li MH. Characterization of activated carbon prepared from chlorella-based algal residue. Bioresour Technol 2015;184:344–8.
[35] Brownlee IA, Allen A, Pearson JP, Dettmar PW, Havler ME, Atherton MR, et al. Alginate as a source of dietary fiber. Crit Rev Food Sci Nutr 2005;45(6):497–510.
[36] Gómez-Díaz D, Navaza JM. Rheology of aqueous solutions of food additives: effect of concentration, temperature and blending. J Food Eng 2003;56(4):387–92.
[37] Tønnesen HH, Karlsen J. Alginate in drug delivery systems. Drug Dev Ind Pharm 2002;28(6):621–30.
[38] Sing KSW, Everett DH, Haul RAW, Moscou L, Pierotti RA, Roquerol J. Reporting physisorption data for gas/solid systems with special reference to the determination of surface area and porosity. Pure Appl Phys Chem 1985;57(4):603–19.
[39] Builes S, Roussel T, Ghimbeu CM, Parmentier J, Gadiou R, Vix-Guterl C, et al. Microporous carbon adsorbents with high CO_2 capacities for industrial applications. Phys Chem Chem Phys 2011;13(35):16063–70.
[40] Cong H, Zhang M, Chen Y, Chen K, Hao Y, Zhao Y, et al. Highly selective CO_2 capture by nitrogen enriched porous carbons. Carbon 2015;92:297–304.
[41] Sun F, Liu X, Gao J, Pi X, Wang L, Qu Z, et al. Highlighting the role of nitrogen doping in enhancing CO_2 uptake onto carbon surfaces: a combined experimental and computational analysis. J Mater Chem 2016;4(47):18248–52.
[42] Chandra V, Yu SU, Kim SH, Yoon YS, Kim DY, Kwon AH, et al. Highly selective CO_2 capture on N-doped carbon produced by chemical activation of polypyrrole functionalized graphene sheets. Chem Commun 2012;48(5):735–7.
[43] Plaza MG, Pevida C, Arias B, Fermoso J, Casal MD, Martín CF, et al. Development of low-cost biomass-based adsorbents for postcombustion CO_2 capture. Fuel 2009;88(12):2442–7.
[44] Casco ME, Martínez-Escandell M, Silvestre-Albero J, Rodríguez-Reinoso F. Effect of the porous structure in carbon materials for CO_2 capture at atmospheric and high-pressure. Carbon 2014;67:230–5.
[45] Presser V, McDonough J, Yeon S-H, Gogotsi Y. Effect of pore size on carbon dioxide sorption by carbide derived carbon. Energy Environ Sci 2011;4(8):3059–66.
[46] Lozano-Castelló D, Cazorla-Amorós D, Linares-Solano A. Powdered activated carbons and activated carbon fibers for methane storage: a comparative study. Energy Fuels 2002;16(5):1321–8.
[47] Vargas DP, Giraldo L, Moreno-Piraján JC. Carbon dioxide and methane adsorption at high pressure on activated carbon materials. Adsorption 2013;19(6):1075–82.
[48] Biloé S, Goetz V, Guillot A. Optimal design of an activated carbon for an adsorbed natural gas storage system. Carbon 2002;40(8):1295–308.
[49] Matranga KR, Myers AL, Glandt ED. Storage of natural gas by adsorption on activated carbon. Chem Eng Sci 1992;47(7):1569–79.
[50] Cracknell RF, Gordon P, Gubbins KE. Influence of pore geometry on the design of microporous materials for methane storage. J Phys Chem 1993;97(2):494–9.
[51] Chen XS, McEnaney B, Mays TJ, Alcaniz-Monge J, Cazorla-Amoros D, Linares-Solano A. Theoretical and experimental studies of methane adsorption on microporous carbons. Carbon 1997;35(9):1251–8.
[52] Lozano-Castelló D, Cazorla-Amorós D, Linares-Solano A, Quinn DF. Influence of pore size distribution on methane storage at relatively low pressure: preparation of activated carbon with optimum pore size. Carbon 2002;40(7):989–1002.